Quantum control in a double well with symmetric or asymmetric driving

Gengbiao Lu, Wenhua Hai,* and Honghua Zhong
Department of Physics and Key Laboratory of Low-Dimensional Quantum Structure and Quantum Control of Ministry of Education, Hunan Normal University, Changsha 410081, China
(Received 3 May 2009; published 21 July 2009)

We investigate the coherent control of a single particle held in a quartic double well with a symmetric or asymmetric driving and exhibit time evolutions of relative probability of the particle in one of the double-well wells. It is shown analytically and numerically that the coherent destruction of tunneling could occur only for the symmetric intense driving, and application of the asymmetric sawtooth driving leads to an increase in the tunneling rate. The results agree with the recent experimental data reported by Kierig *et al.* [Phys. Rev. Lett. **100**, 190405 (2008)]. We also exhibit the effect of multiple photon resonances on the tunneling through a dc field. Finally, we demonstrate a connection between the classically chaotic barrier crossing and quantum tunneling numerically.

DOI: 10.1103/PhysRevA.80.013411 PACS number(s): 32.80.Qk, 32.80.Wr, 42.50.Hz, 03.65.Ge

I. INTRODUCTION

Research on the coherent control of quantum tunneling with time-dependent external field has been a subject of recent theoretical and experimental works [1–7]. A single particle in a quartic double well consisting of two wells and driven by a monochromatic periodical field is a typical system to demonstrate the coherent control. Previously, Lin and Ballentine [8] proved that the tunneling rate can be highly enhanced due to the periodic modulations associated with chaos. Then Grossmann *et al.* [9] found another peculiar effect, namely, when the strength and frequency of the periodic driving are chosen appropriately, a particle initially located in one of the two wells never transfers to the other, which is called the "coherent destruction of tunneling" (CDT). Bavli and Metiu [10] showed that a semi-infinite monochromatic driving also can be used to localize an electron in one of the double-well wells. Farrelly and Milligan [11] further exhibited that the control of tunneling can be achieved by a two-frequency driving with frequency ratio 1:2. Recently, Kierig *et al.* [6] reported the first direct observation of the coherent control of single-particle tunneling in a strongly driven double-well potential. Periodic arrangement of the double well is achieved by employing the standard optical light shift potential and an atom of argon is prepared in one well initially. The momentum distribution is given and the tunneling effect is directly shown up in the dynamics of the diffraction efficiencies. The experimental results reveal that the symmetric driving suppresses the tunneling and the asymmetric sawtooth driving raises the rate of tunneling.

In this paper, we investigate the coherent control of quantum tunneling in the experiment reported in Ref. [6] by using the perturbation analysis and nonperturbed numerical method. It is shown that the CDT can occur only for the symmetric intense driving and application of the asymmetric two-frequency sawtooth driving leads to increase in the tunneling rate. Our results are in good agreement with the recent experimental data [6]. We also reveal the effect of multiple photon resonances on the tunneling through a dc field. Finally, we illustrate a connection between the classical chaos and quantum tunneling and find a good correspondence between the classically chaotic barrier crossing and quantum tunneling numerically through the Poincaré sections on classical phase space.

II. HIGH-FREQUENCY AND WEAK-COUPLING APPROXIMATION

For a single particle confined in the double-well traps, we focus on the lowest doublet of energy eigenstates, which are composed of the linear combinations of low-lying state pairs localized in the left and the right wells [12]. When the modulation amplitude of the energies of the left and right wells is much smaller than the representative excitation energy in a single well, the tunneling dynamics of the system in Ref. [6] can be described by the two-level model [13,14]. The corresponding dimensionless Hamiltonian reads

$$H(t) = \frac{\varepsilon(t)}{2}(|1\rangle\langle 1| - |2\rangle\langle 2|) + \Omega(|1\rangle\langle 2| + |2\rangle\langle 1|),$$

$$\varepsilon(t) = \varepsilon_0 - \varepsilon_1 \sin(\omega t + \theta_1) - \varepsilon_2 \sin(2\omega t + \theta_2), \qquad (1)$$

where $|1\rangle$ and $|2\rangle$ represent the left and the right localized states in the double-well system; $\varepsilon(t)$ denotes the time-dependent external field with ω being the driving frequency and $\theta_j (j=1,2)$ being the phases, ε_0 is the dc field strength, ε_1 and ε_2 are the driving strengths, and Ω is the tunneling coefficient between the two wells, which represents the gain in kinetic energy in a tunneling event. For simplification, we have set $\hbar = 1$ and normalized energy and time by ω_0 and ω_0^{-1} with ω_0 being a fixed reference frequency. The parameters $\varepsilon_j (j=0,1,2)$, Ω, and ω are in units of ω_0. Thus all the parameters are dimensionless throughout this paper.

The quantum system (1) is described by the wave function $\Psi(t)$ which can be expanded in the basis $|1\rangle$ and $|2\rangle$ as

$$|\Psi(t)\rangle = \alpha_1(t)|1\rangle + \alpha_2(t)|2\rangle, \qquad (2)$$

where $\alpha_1(t)$ and $\alpha_2(t)$ are the time-dependent dimensionless coefficients. Applying Eqs. (1) and (2) to the Schrödinger

*Corresponding author; whhai2005@yahoo.com.cn

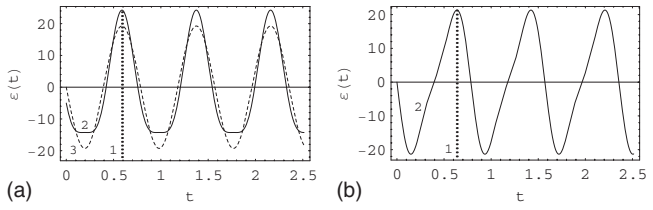

FIG. 1. (a) Time evolutions of the driving function $\varepsilon(t)$ for the symmetric two-frequency field (curve 2) and single-frequency field (curve 3). (b) Time evolution of the asymmetric two-frequency driving field (curve 2). Line 1 in both figures stands for the perpendicular line. The driving function and time are dimensionless.

equation $i\frac{\partial}{\partial t}|\Psi(t)\rangle = H(t)|\Psi(t)\rangle$ results in the coupled equations

$$i\dot{\alpha}_1(t) = \frac{\varepsilon(t)}{2}\alpha_1(t) + \Omega\alpha_2(t), \tag{3}$$

$$i\dot{\alpha}_2(t) = -\frac{\varepsilon(t)}{2}\alpha_2(t) + \Omega\alpha_1(t). \tag{4}$$

It is difficult for us to obtain the exact solutions of Eqs. (3) and (4). However, under the weakly coupled condition $\Omega \ll 1$, we can construct the perturbation solutions as follows. Setting $\alpha_1(t)=b_1(t)\exp[-\frac{i}{2}\int_0^t\varepsilon(t)dt]$ and $\alpha_2(t)=b_2(t)\exp[\frac{i}{2}\int_0^t\varepsilon(t)dt]$ and inserting them into Eqs. (3) and (4), we obtain $i\dot{b}_1=\Omega b_2\exp[i\int_0^t\varepsilon(t)dt]$, $i\dot{b}_2=\Omega b_1\exp[-i\int_0^t\varepsilon(t)dt]$. We then consider the perturbed corrections up to the first-order approximation $b_j=b_j^{(0)}+b_j^{(1)}$ with $|b_j^{(1)}| \ll |b_j^{(0)}|$ for $j=1,2$. Clearly the zero-order solutions $b_j^{(0)}=c_j$ are the constants decided by initial conditions and the first-order solutions obey the decoupled equations

$$i\dot{b}_1^{(1)} = \Omega c_2 \exp\left[i\int_0^t \varepsilon(t)dt\right], \tag{5}$$

$$i\dot{b}_2^{(1)} = \Omega c_1 \exp\left[-i\int_0^t \varepsilon(t)dt\right]. \tag{6}$$

In the high-frequency approximation, when $\varepsilon_0=\varepsilon_2=0$ is set, from Eqs. (5) and (6) the effective tunneling coefficient can be reduced to [13] $\Omega J_0(\frac{\varepsilon_1}{\omega})$ with $J_0(\frac{\varepsilon_1}{\omega})$ being the zeroth-order ordinary Bessel function. Thus the CDT can be clearly seen for the appropriate parameters ε_1/ω fitting $J_0(\frac{\varepsilon_1}{\omega})=0$. For the single-frequency field case such a result is consistent with the corresponding result [9] from the Floquet analysis with the tunneling splitting $\Delta_{eff}=\Delta J_0(\frac{\varepsilon_1}{\omega})$. We here are interested in the two-frequency driving and nonzero dc field cases.

For the nonzero ε_j $(j=1,2)$, the time-evolution curves of the driving $\varepsilon(t)$ may be symmetric or asymmetric depending on the values of strengths and phases. In Fig. 1, we exhibit the temporal symmetry and asymmetry for different driving parameters. Curve 2 of Fig. 1(a) stands for the time evolution of symmetric two-frequency driving field for the parameters $\omega=8$, $\varepsilon_0=0$, $\varepsilon_1=19.26$, $\varepsilon_2=5$, $\theta_1=0$, $\theta_2=0.5\pi$. Taking $\varepsilon_2=0$ we transform curve 2 to curve 3 related to the symmetric single-frequency driving. The parameters of Fig. 1(b) are the same as that of curve 2 in Fig. 1(a), except $\theta_2=0$. Curve 2 of Fig. 1(b) denotes the time evolution of two-frequency asymmetrical driving, which is similar to the sawtooth driving in the single-particle experiment [6]. The symmetry of driving field is embodied by the perpendicular line 1 in both the figures. We will investigate the coherent control for the above two symmetric drives and one asymmetric drive, respectively, as follows.

A. Case 1

This shows the single-frequency symmetric driving of Eq. (1) with $\theta_1=0$ and $\varepsilon_2=0$. Such a field is a simple sine function of time, which is plotted as curve 3 in Fig. 1(a). Applications of such a function and the Fourier expansion $\exp[\pm ix\cos(\omega t)]=\Sigma_{n'=-\infty}^{\infty}J_{n'}(x)(\pm i)^{n'}\exp(in'\omega t)$ lead to the expansion formula $\exp[\pm i\int\varepsilon(t)dt]=\Sigma_{n'=-\infty}^{\infty}J_{n'}(\frac{\varepsilon_1}{\omega})(\pm i)^{n'}\exp[i(n'\omega\pm\varepsilon_0)t]$, where $J_{n'}(x)$ is the n'-order Bessel function. Substituting the formula into Eqs. (5) and (6) and setting $\varepsilon_0=n\omega+\delta$ with $|\delta|\leq\frac{\omega}{2}$ and n integer, under the high-frequency approximation $\omega\gg 1$, we obtain the solutions

$$b_1^{(1)} \approx -i^{-n}c_2'\Omega J_{-n}\left(\frac{\varepsilon_1}{\omega}\right)\frac{e^{i\delta t}-1}{\delta}, \tag{7}$$

$$b_2^{(1)} \approx (-i)^{-n}c_1'\Omega J_{-n}\left(\frac{\varepsilon_1}{\omega}\right)\frac{e^{-i\delta t}-1}{\delta}, \tag{8}$$

where $c_1'=c_1e^{i\varepsilon_1/\omega}$ and $c_2'=c_2e^{-i\varepsilon_1/\omega}$. Hereafter, we call δ the "reduced strength" of the dc field. The result implies that the tunneling parameter Ω is replaced by the effective one $\Omega_{eff}=\Omega J_{-n}(\frac{\varepsilon_1}{\omega})$ and the effective tunneling rate reads Ω_{eff}/Ω [15]. Therefore we can set the appropriate driving parameters (ε_1,ω) to make $J_{-n}(\frac{\varepsilon_1}{\omega})=0$ such that the effective tunneling rate vanishes. The zero Ω_{eff} means that $b_j^{(1)}=0$ and $|\alpha_j|^2=|b_j^{(0)}|^2=|c_j|^2$ for $j=1,2$, namely, the probabilities of the particle in every well are constants. Thus the particle will be maintained in the initially localized state and no quantum tunneling occurs. The results well agree with the corresponding CDT experiment [6].

We now see the effect of multiple photon resonance [15–17] induced by condition $\varepsilon_0=n\omega$ or $\delta=0$. When $\delta\to 0$ is set, the application of l'Hospital rule to Eqs. (7) and (8) leads to linear increase in the solutions with time, $b_j^{(1)}\propto t$, which indicate the appearance of resonance tunneling. In fact, we can prepare the particle in the first well initially with $c_1=1$, $c_2=c_2'=0$ and from Eqs. (7) and (8) derive $b_1^{(1)}=0$ and $b_2^{(1)}\propto t$ so that the tunneling from the first well to the second well will occur with linearly increasing amplitude. For the nonzero δ, $b_j^{(1)}$ for $j=1,2$ are two periodic functions of time, which means that ground-state levels of the two wells are shifted out of resonance and the linear increase in tunneling amplitude is suppressed. The results are similar to the recent experiment observations of photon-assisted tunneling in optical lattice [15].

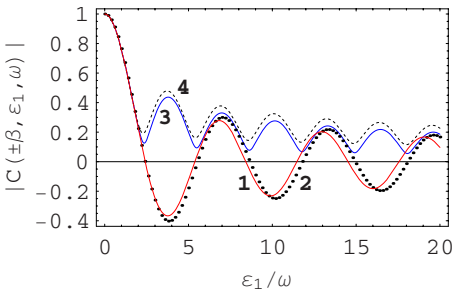

FIG. 2. (Color online) The evolution of function $|C(\pm\beta,\varepsilon_1,\omega)|$ versus $\frac{\varepsilon_1}{\omega}$ for $\beta=1$ (curve 1) and $\beta=i$ (curves 3 and 4) with $\varepsilon_1=4\varepsilon_2$ (curves 1, 2, and 3) and $\varepsilon_1=3\varepsilon_2$ (curve 4). The dotted line 2 stands for the Bessel function $J_0(\frac{\varepsilon_1}{\omega})$. The other parameters are chosen as $\varepsilon_0=0$, $\varepsilon_1=19.26$, $\omega=8$. The dimensionless quantities and parameters are used.

B. Case 2

The two-frequency symmetric driving of Eq. (1) with $\varepsilon_0=0$, $\theta_1=0$, and $\theta_2=0.5\pi$ is associated with the curve 2 in Fig. 1(a). Applying Fourier expansion of the functions $\exp[\pm i\frac{\varepsilon_1}{\omega}\cos(\omega t)]$ and $\exp[\pm i\frac{\varepsilon_2}{\omega}\sin(2\omega t)]$, we obtain the expansion formula $\exp[\pm i\int\varepsilon(t)dt]=\Sigma_{n'=-\infty}^{\infty}\Sigma_{m=-\infty}^{\infty}J_{n'}(\frac{\varepsilon_1}{\omega})J_m(\frac{\varepsilon_2}{\omega})(\pm i)^{n'}(\pm 1)^m\exp[i(n'+2m)\omega t]$. In the high-frequency case with $\omega\gg 1$ and after substituting the expansion formula into Eqs. (5) and (6), we integrate them and neglect the unimportant oscillating terms which are inversely proportional to ω, producing the approximate solutions with $n'+2m=0$,

$$b_1^{(1)}\approx -id_2\Omega C(\beta,\varepsilon_1,\varepsilon_2,\omega)t, \tag{9}$$

$$b_2^{(1)}\approx -id_1\Omega C(-\beta,\varepsilon_1,\varepsilon_2,\omega)t, \tag{10}$$

$$C(\pm\beta,\varepsilon_1,\varepsilon_2,\omega)=\sum_m(\pm\beta)^{-m}J_{-2m}\left(\frac{\varepsilon_1}{\omega}\right)J_m\left(\frac{\varepsilon_2}{2\omega}\right) \tag{11}$$

with the constants $\beta=1$, $d_1=c_1e^{i\varepsilon_1/\omega}$, and $d_2=c_2e^{-i\varepsilon_1/\omega}$. In Eqs. (9) and (10), the dimensionless coefficients $C(\pm 1,\varepsilon_1,\varepsilon_2,\omega)$ are real numbers for a set of fixed parameters. Although these are in the resonance case ($\varepsilon_0=0$), CDT may occur for some appropriate parameters. In order to illustrate CDT, we take $\varepsilon_1=4\varepsilon_2$ that leads $C(\pm 1,\varepsilon_1,\varepsilon_2,\omega)=|C(\pm 1,\varepsilon_1,\omega)|$ to the function of $\frac{\varepsilon_1}{\omega}$. The evolution of $|C(\pm 1,\varepsilon_1,\omega)|$ versus $\frac{\varepsilon_1}{\omega}$ is plotted as curve 1 of Fig. 2. From this curve we can see that at appropriate values of the parameter ratio $\frac{\varepsilon_1}{\omega}$, $C(\pm 1,\varepsilon_1,\omega)$ vanishes, which means $b_j^{(1)}=0$ for $j=1,2$ and the particle will be maintained in the initially localized state. The result indicates the CDT can be realized under the two-frequency symmetrical driving. In the meantime, we find that the evolution of the coefficient $C(\pm 1,\varepsilon_1,\omega)$ versus $\frac{\varepsilon_1}{\omega}$ (the curve 1) is similar to that of the Bessel function $J_0(\frac{\varepsilon_1}{\omega})$ (the dotted line 2) in Eqs. (7) and (8) for $\varepsilon_0=0$ and $\varepsilon_1=4\varepsilon_2$, which demonstrate the similar characteristic between single-frequency and two-frequency symmetrical driving fields.

Based on the semiclassical Husimi-function method, for the two-frequency driving field of Eq. (1) with $\theta_1=\theta_2=0.5\pi$, Farrelly *et al.* [11] have reported the result on the suppression of tunneling. A similar result can be easily established by the above full quantum-mechanical treatment because of the temporal symmetry of driving field in such a case.

C. Case 3

The two-frequency asymmetric driving of Eq. (1) with $\varepsilon_0=0$ and $\theta_1=\theta_2=0$ corresponds to the curve 2 in Fig. 1(b). The similar calculations to case 2 give the high-frequency approximate solutions of Eqs. (5) and (6) as

$$b_1^{(1)}\approx -ie_2\Omega C(\beta,\varepsilon_1,\varepsilon_2,\omega)t, \tag{12}$$

$$b_2^{(1)}\approx -ie_1\Omega C(-\beta,\varepsilon_1,\varepsilon_2,\omega)t, \tag{13}$$

with the constants $e_1=c_1e^{i2\varepsilon_1+\varepsilon_2/2\omega}$ and $e_2=c_2e^{-i2\varepsilon_1+\varepsilon_2/2\omega}$. Here coefficients $C(\pm\beta,\varepsilon_1,\varepsilon_2,\omega)$ are defined by Eq. (11) for $\beta=i$, which are two complex numbers with the same module. Adopting the similar selection $\varepsilon_1=4\varepsilon_2$ with case 2, we plot the evolution of the module $|C(\pm i,\varepsilon_1,\varepsilon_2,\omega)|=|C(\pm i,\varepsilon_1,\omega)|$ versus $\frac{\varepsilon_1}{\omega}$ as the curve 3 of Fig. 2, and no zero point is observed for any ratio $\frac{\varepsilon_1}{\omega}$. After changing ε_1 from $4\varepsilon_2$ to $3\varepsilon_2$, curve 3 of Fig. 2 is transformed to curve 4 on which also no zero point is found. Further for the asymmetric drive case we take many different groups of parameters to plot $|C(\pm i,\varepsilon_1,\omega)|$ and still do not observe any zero point. So the solutions in Eqs. (12) and (13) will linearly increase with time that indicates the appearance of resonance tunneling. The result means that the CDT cannot occur under the asymmetrical sawtooth-driving field. This is in good agreement with the recent experimental data [6].

III. NUMERICAL RESULTS FROM EXACT MODEL

Under the high-frequency and weak-coupling approximation, the analytical results given by Eqs. (7)–(13) describe the coherent control of quantum tunneling well for the single-frequency and two-frequency driving fields. Further, we are interested in (a) the comparison between the analytical and numerical results, and (b) the numerical results without the high-frequency and weak-coupling approximation. We will seek general results of the coherent control, through the numerical analysis from exact Eqs. (3) and (4). Setting $\alpha_j=\sqrt{\lambda_j}e^{i\theta_j}$, $j=1,2$ and $z=\lambda_2-\lambda_1$, $\phi=\theta_2-\theta_1$, and considering the orthonormalization condition $\lambda_1+\lambda_2=1$, Eqs. (3) and (4) are rewritten as

$$\dot{z}=-2\Omega\sqrt{1-z^2}\sin\phi, \tag{14}$$

$$\dot{\phi}=\varepsilon(t)+\frac{2\Omega z}{\sqrt{1-z^2}}\cos\phi, \tag{15}$$

where z is the relative probability of single particle in one well and ϕ the phase difference. The particle is localized in the first well for $z=1$ and in the second well for $z=-1$. Based on Eqs. (14) and (15), we will explore the tunneling dynam-

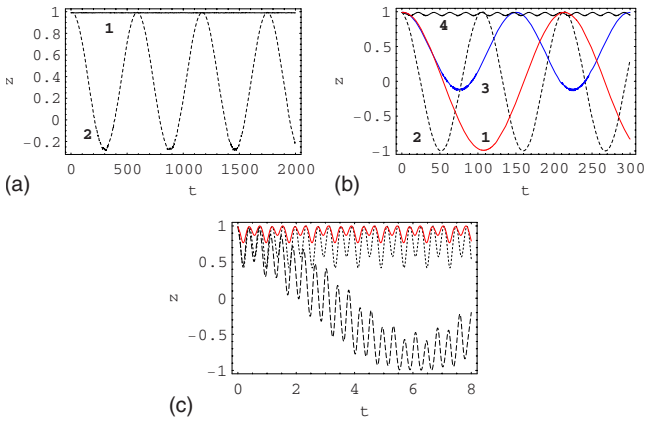

FIG. 3. (Color online) (a) The time evolutions of z for the parameters $\varepsilon_2=0$, $\theta_1=0$, $\varepsilon_0=0.007$, $\Omega=0.05$, $\omega=8$ and the different strengths of driving fields $\varepsilon_1=19.238$ (curve 1) and $\varepsilon_1=18$ (curve 2). (b) The time evolutions of z for the parameters $\varepsilon_2=0$, $\Omega=0.05$, $\omega=8$, $\varepsilon_1=15$, $\theta_1=0$ and the different strengths of static electric fields $\varepsilon_0=0$ (curve 1), $\varepsilon_0=8$ (curve 2), $\varepsilon_0=0.03$ (curve 3), and $\varepsilon_0=0.3$ (curve 4). (c) The time evolutions of z for the parameters $\theta_1=0$, $\omega=8$, $\varepsilon_0=0$, $\varepsilon_2=0$, and the different parameter pairs $\Omega=2$, $\varepsilon_1=18.65$ (solid curve), $\Omega=3.5$, $\varepsilon_1=18.65$ (long dashed curve), and $\Omega=3.5$, $\varepsilon_1=17.30$ (dotted curve). The relative probability z and time t are dimensionless.

ics numerically for the symmetrical and asymmetrical driving fields as follows.

First, we consider the single-frequency driving of Eq. (1) with parameters $\varepsilon_0=0.007$ and $\varepsilon_2=0$ and the high-frequency and weak-coupling case with $\omega=8$, $\Omega=0.05$, and $\theta_1=0$. For two different values of driving strength ε_1, we plot the time evolutions of z as in Fig. 3(a). From this figure we observe that at the zero-point $\frac{\varepsilon_1}{\omega}=2.404\,75$ of Bessel function $J_0(\frac{\varepsilon_1}{\omega})$ the relative probability z maintains the initial value (curve 1) that means the occurrence of CDT. However, when the parameter ratio $\frac{\varepsilon_1}{\omega}$ deviates from the zero point of Bessel function $J_0(\frac{\varepsilon_1}{\omega})$, z oscillates in time with the largest amplitude $z_{max}=1$ as curve 2 of Fig. 3(a) with $\frac{\varepsilon_1}{\omega}=2.25$ that indicates the periodic quantum tunneling, namely, periodic population oscillation. The numerical results are in good agreement with the analytical ones from Eqs. (7) and (8).

Similarly, we consider the high-frequency, weak-coupling, and single-frequency driving case with parameters $\omega=8$, $\Omega=0.05$, $\theta_1=0$, $\varepsilon_2=0$, $\varepsilon_1=15$ to exhibit the time evolutions of z for different dc field strength ε_0 as in Fig. 3(b). For the strength values $\varepsilon_0=n\omega$ with $n=0,1$, from curves 1 and 2 of Fig. 3(b) we find that the periodic tunneling of the largest amplitude $z_{max}=1$ occurs in both cases. But $n=1$ case (curve 2) possesses smaller tunneling period compared to $n=0$ case (curve 1) which implies the former having larger tunneling rate. This result is very important for one to design an atom device [18]. It should be noticed that after considering the normalization, the multiple photon resonances with $\varepsilon_0=n\omega$ result in the largest amplitude of z. For the nonzero reduced strength values $\varepsilon_0=\delta=0.03,0.3$, from curve 3 and curve 4 of Fig. 3(b) we find that the amplitude of z is suppressed and the larger strength value corresponds to the smaller amplitude. The result is similar to the experimental result in optical lattice [15].

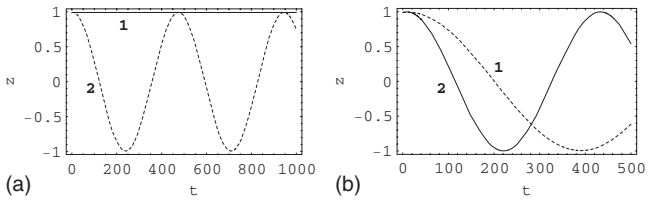

FIG. 4. The time evolutions of z for $\Omega=0.05$, $\omega=8$, $\varepsilon_0=0$, $\varepsilon_2=5$, $\theta_1=0$ and the different parameter pairs (a) $\varepsilon_1=19.2638$, $\theta_2=0.5\pi$ (curve 1) and $\varepsilon_1=19.2638$, $\theta_2=0$ (curve 2). (b) $\varepsilon_1=18$, $\theta_2=0.5\pi$ (curve 1) and $\varepsilon_1=18$, $\theta_2=0$ (curve 2). Here z and t are dimensionless.

In the strong-couple and single-frequency driving case, from Eqs. (14) and (15) we also can explore the quantum tunneling of particle. In Fig. 3(c) we show the time evolutions of relative probability z for two different tunneling coefficients $\Omega=2$ (solid curve) and $\Omega=3.5$ (long dashed curve) for the same potential parameters $\varepsilon_1=18.65$, $\varepsilon_2=0$, $\omega=8$. From the solid curve with $\Omega=2$ we observe the small oscillations of z. We also find that the increase in tunneling coefficient Ω (from 2 to 3.5) leads the region of z evolution to obviously increase. Keeping $\Omega=3.5$ and decreasing the field strength to $\varepsilon_1=17.30$, the amplitude of z is decreased again, which is exhibited by the dotted curve with amplitude being less than that of the long dashed curve case but greater than that of the solid curve case. The result indicates that no CDT occurs for any strong-couple and single-frequency driving case.

Now we illustrate numerically that the CDT could occur only for the symmetric driving. In Fig. 4(a), for the parameters $\omega=8$, $\Omega=0.05$, $\varepsilon_0=0$, $\varepsilon_1=19.26$, $\varepsilon_2=5$, we display the time evolutions of z for two-frequency symmetric ($\theta_1=0$, $\theta_2=0.5\pi$) and asymmetric ($\theta_1=\theta_2=0$) drives. The curve 1 stands for the time evolution of relative probability z in symmetrical driving, where the relative probability z approximately keeps the initial value $z=1$. The curve 2 indicates the time oscillations of z in asymmetrical driving with the largest amplitude $|z|_{max}=1$. The numerical results agree well with the above-mentioned analytical results.

Further, we explore the resonance tunneling rate numerically for the parameters $\theta_1=0$, $\omega=8$, $\Omega=0.05$, $\varepsilon_0=0$, $\varepsilon_1=18$, $\varepsilon_2=5$ and the two-frequency symmetric ($\theta_2=0.5\pi$) and asymmetric ($\theta_2=0$) driving fields. In Fig. 4(b), we see the periodic oscillations of z and reveal that the application of the asymmetric driving can lead to increase in the tunneling rate. It is shown that the asymmetry case with $\theta_2=0$ (curve 2) has smaller oscillating period of z compared to the symmetry case with $\theta_2=0.5\pi$ (curve 1) that means the former corresponding to higher tunneling rate. The results agree well with the recent experimental one [6].

To see the coherent control from different viewpoints, from Eqs. (14) and (15) we give the orbits of phase space $z\_\dot{z}$ numerically as in Fig. 5. In Figs. 5(a) and 5(b) we show that the single-frequency and two-frequency symmetric driving fields can well suppress the change in relative probability z in the small region $0.993<z<1$. However, the asymmetric driving leads the oscillation amplitude of z to the greatest one $-1\leq z\leq 1$ as in Fig. 5(c). This demonstrates again that

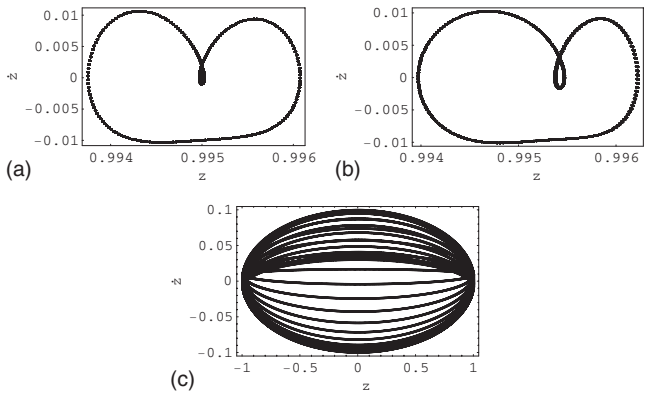

FIG. 5. The orbits of phase space of dimensionless phase variables $z,\dot{z}$. The parameters are chosen as $\theta_1=0$, $\Omega=0.05$, $\omega=8$, $\varepsilon_0=0$, $\varepsilon_1=19.238$ and (a) $\varepsilon_2=0$; (b) $\varepsilon_2=5$, $\theta_2=0.5\pi$; (c) $\varepsilon_2=5$, $\theta_2=0$.

the suppression of tunneling can be achieved only for the symmetrical driving.

Finally, we seek the connection between classical chaos and the quantum tunneling. The classical Hamiltonian corresponding to quantum system (1) reads $H(x,t)=\frac{p^2}{2}+V(x)+\frac{x}{d}\varepsilon(t)$ [12], where $V(x)=Bx^4-Dx^2$ is the symmetric double-well potential and d is the distance between the bottom of a well and symmetric center of the double-well wells. We choose the well parameters $B=0.5\hbar\omega_0/(\mu\text{m})^4$ and $D=10\hbar\omega_0/(\mu\text{m})^2$ and the distance $2d=2\sqrt{10}$ μm between two wells. To make a comparison between classical and quantum motions, we employ the symmetric and asymmetric driving fields of Fig. 1 and the initial conditions $x(t_0)=-2.5$ μm, $\dot{x}(t_0)=4.5\omega_0$ μm (the particle being in the left well initially) to plot the Poincaré sections of the phase space $x\_\dot{x}$ as in Fig. 6, where t_0 denotes the initial time. It is very interesting noting that for the single-frequency [Fig. 6(a)] and two-frequency [Fig. 6(b)] symmetric driving fields the particle being initially in the left well $[x(t_0)<0]$ keeps in the same well $[x(t)<0]$ for any $t>t_0$. The corresponding phase orbits are similarly regular for the both cases. However, for the two-frequency asymmetric field [Fig. 6(c)] the particle can cross the barrier between the two wells to reach the right well with $x(t)>0$. The numerical orbit in Fig. 6(c) seems to be chaotic that agrees with the result of chaos-induced tunneling in Ref. [8]. Here, we demonstrate a good correspondence between the classical barrier crossing and quantum tunneling, which are affected similarly by the symmetric or asymmetric driving field. The classical overbarrier in Fig. 6(c) could be associated with the instability of chaos, and its quantum correspondence should be related not only to the lower two states, but also to the higher quantum levels of the system. The result is helpful for us to further understand the connection between quantum tunneling and classical chaos in a double-well system [8,19].

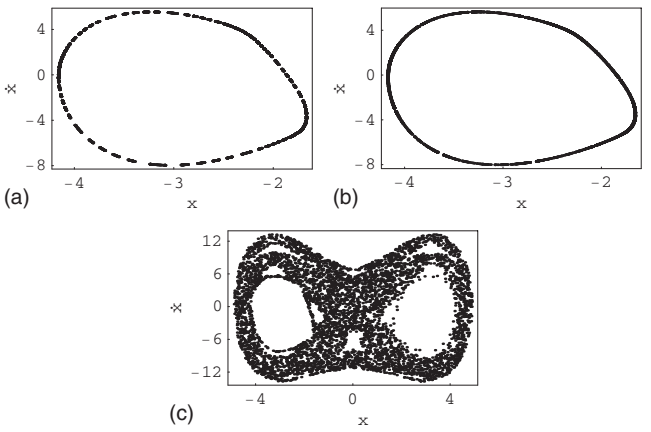

FIG. 6. The Poincaré surfaces of section for different driving fields. The parameters are chosen as $B=0.5$, $D=10$, $x_0=-2.5$, $\dot{x}_0=4.5$, and (a) $\theta_1=0$, $\omega=8$, $\varepsilon_0=0$, $\varepsilon_1=19.26$, $\varepsilon_2=0$; (b) $\theta_1=0$, $\omega=8$, $\varepsilon_0=0$, $\varepsilon_1=19.26$, $\varepsilon_2=5$, $\theta_2=0.5\pi$; (c) $\theta_1=0$, $\omega=8$, $\varepsilon_0=0$, $\varepsilon_1=19.26$, $\varepsilon_2=5$, $\theta_2=0$. The system parameters are in the same units with that of Fig. 1, and x and $\dot{x}$ are in units μm and $\omega_0\mu$m.

IV. CONCLUSION

By using the perturbation analysis and nonperturbative numerical method, we have investigated the coherent control for the single particle held in the double-well wells and driven by the time-dependent symmetric or asymmetric field. The time evolutions of relative probability of the particle in each well are illustrated, by which we demonstrate analytically and numerically the critical dependence of CDT on the underlying symmetry of the driving field. It is revealed that the CDT can occur only for the symmetric driving and the application of the asymmetric sawtooth driving leads to increase in the tunneling rate. We also exhibit the effect of multiple photon resonances on the tunneling through the dc field with strength ε_0. It is shown that the tunneling rate could be enhanced by increasing the multiple n under the resonance condition $\varepsilon_0=n\omega$ and the amplitude of relative probability can be suppressed by adjusting the reduced strength δ of the dc field for the nonresonance case $\varepsilon_0=n\omega+\delta$. Finally, we demonstrate the connection between quantum tunneling and classical chaos and find the correspondence between the classical barrier crossing and quantum tunneling. The results are in good agreement with the recent experimental data reported in Ref. [6] and can be easily extended to the case of a particle held in a chain of coupled double-well wells [20].

ACKNOWLEDGMENTS

This work was supported by the National Natural Science Foundation of China under Grants No. 10575034 and No. 10875039 and supported by Construct Program of the National Key Discipline.

[1] P. Kral, Rev. Mod. Phys. **79**, 53 (2007).
[2] M. Grifoni and P. Hsnhhi, Phys. Rep. **304**, 229 (1998); I. Vorobeichik and N. Moiseyev, Phys. Rev. A **59**, 2511 (1999).
[3] Q. Xie and W. Hai, Phys. Rev. A **75**, 015603 (2007); H. Zhong, W. Hai, and S. Rong, J. Phys. B **41**, 175301 (2008).
[4] X. Luo, Q. Xie, and B. Wu, Phys. Rev. A **76**, 051802(R) (2007).
[5] G. DellaValle, M. Ornigotti, E. Cianci, V. Foglietti, P. Laporta, and S. Longhi, Phys. Rev. Lett. **98**, 263601 (2007).
[6] E. Kierig, U. Schnorrberger, A. Schietinger, J. Tomkovic, and M. K. Oberthaler, Phys. Rev. Lett. **100**, 190405 (2008).
[7] S. Longhi, Phys. Rev. B **77**, 195326 (2008).
[8] W. A. Lin and L. E. Ballentine, Phys. Rev. Lett. **65**, 2927 (1990); G. M. D'Ariano, L. R. Evangelista, and M. Saraceno, Phys. Rev. A **45**, 3646 (1992).
[9] F. Grossmann, T. Dittrich, P. Jung, and P. Hanggi, Phys. Rev. Lett. **67**, 516 (1991); G. Großmann and P. Hänggi, Europhys. Lett. **18**, 571 (1992).
[10] R. Bavli and H. Metiu, Phys. Rev. Lett. **69**, 1986 (1992).
[11] D. Farrelly and J. A. Milligan, Phys. Rev. E **47**, R2225 (1993).
[12] T. Jinasundera, C. Weiss, and M. Holthaus, Chem. Phys. **322**, 118 (2006).
[13] J. M. Gomez Llorente and J. Plata, Phys. Rev. A **45**, R6958 (1992); Y. Kayanuma, *ibid.* **50**, 843 (1994).
[14] Y. Kayanuma and K. Saito, Phys. Rev. A **77**, 010101(R) (2008).
[15] C. Sias, H. Lignier, Y. P. Singh, A. Zenesini, D. Ciampini, O. Morsch, and E. Arimondo, Phys. Rev. Lett. **100**, 040404 (2008).
[16] M. Holthaus, G. H. Ristow, and D. W. Hone, Phys. Rev. Lett. **75**, 3914 (1995).
[17] C. E. Creffield and T. S. Monteiro, Phys. Rev. Lett. **96**, 210403 (2006).
[18] Z. Kim, V. Zaretskey, Y. Yoon, J. F. Schneiderman, M. D. Shaw, P. M. Echternach, F. C. Wellstood, and B. S. Palmer, Phys. Rev. B **78**, 144506 (2008).
[19] Q. Xie, W. Hai, and G. Chong, Chaos **13**, 801 (2003); W. Hai, C. Lee, G. Chong, and L. Shi, Phys. Rev. E **66**, 026202 (2002).
[20] C. E. Creffield, Phys. Rev. Lett. **99**, 110501 (2007).